

## Effect of arylamine hole-transport units on the performance of blue polyspirobifluorene light-emitting diodes

Davood Abbaszadeh,<sup>1,2</sup> Herman T. Nicolai,<sup>3</sup> N. Irina Crăciun,<sup>4</sup> and Paul W. M. Blom<sup>4,5</sup>

<sup>1</sup>*Molecular Electronics, Zernike Institute for Advanced Materials, University of Groningen, Nijenborgh 4, NL-9747AG Groningen, The Netherlands*

<sup>2</sup>*Dutch Polymer Institute, P.O. Box 902, 5600 AX Eindhoven, The Netherlands*

<sup>3</sup>*TNO/Holst Centre, High Tech Campus 31, 5605 KN Eindhoven, The Netherlands*

<sup>4</sup>*Max-Planck Institute for Polymer Research, Ackermannweg 10, Mainz D55128, Germany*

<sup>5</sup>*King Abdulaziz University, Faculty of Science, Physics Department, 22254 Jeddah, Saudi Arabia*

(Received 29 May 2014; revised manuscript received 28 August 2014; published 5 November 2014)

The operation of blue light-emitting diodes based on polyspirobifluorene with a varying number of  $N, N, N', N'$  tetraaryldiamino biphenyl (TAD) hole-transport units (HTUs) is investigated. Assuming that the electron transport is not affected by the incorporation of TAD units, model calculations predict that a concentration of 5% HTU leads to an optimal efficiency for this blue-emitting polymer. However, experimentally an optimum performance is achieved for 10% TAD HTUs. Analysis of the transport and recombination shows that polymer light-emitting diodes with 5%, 7.5%, and 12.5% TAD units follow the predicted behavior. The enhanced performance of the polymer with 10% TAD originates from a decrease in the number of electron traps, which is typically a factor of three lower than the universal value found in many polymers. This reduced number of traps leads to a reduction of nonradiative recombination and exciton quenching at the cathode.

DOI: [10.1103/PhysRevB.90.205204](https://doi.org/10.1103/PhysRevB.90.205204)

PACS number(s): 72.80.Le, 72.20.Jv

### I. INTRODUCTION

Since the discovery of the conducting properties of conjugated polymers, their electronic applications have been investigated extensively. Many conjugated polymers can be processed from solution, enabling cheap deposition methods such as coating and printing. As a result light-emitting diodes (LEDs), solar cells, and transistors made of these polymers have gained much interest also for flexible products. To fabricate efficient polymer light-emitting diodes (PLEDs), it is crucial to understand how they function to optimize their efficiency; therefore, studying their charge transport properties is important. For PLEDs based on poly(p-phenylene vinylene) (PPV) derivatives, it has recently been shown that the hole transport is governed by trap-free space-charge-limited conduction (SCLC), with the mobility dependent on the electric field and charge-carrier density. The electron transport is hindered by the presence of a universal electron trap with a typical density of  $\sim 3\text{--}5 \times 10^{23} \text{ m}^{-3}$  [1]. The trapped electrons recombine with free holes via a nonradiative trap-assisted recombination process, which is a competing loss process with respect to the emissive bimolecular Langevin recombination. Both the Langevin and trap-assisted recombination are governed by the diffusion of the free carrier(s). Therefore, with the charge carrier mobilities and number of trapping centers known from charge transport measurements the radiative recombination, as well as nonradiative loss processes and thus the efficiency of PLEDs, can be fully predicted [2,3].

Among the wide range of polymers, polyfluorenes (PFs) are interesting due to their wide band gap and high efficiency [4,5]. Functionalizing this polymer in different structures has led researchers to optimize their stability and efficiency. Polyspirobifluorene (PSF) is a polymer from the PFs family in which the spiro-center (C-9 atom) links two PF units to each other, making the polymer more stable and more efficient for light emission [6]. To make efficient PLEDs, balanced injection of

holes and electrons is needed. Polyfluorene derivatives mostly have deep highest occupied molecular (HOMO) level in comparison to conventional hole injecting materials like indium tin oxide (ITO) and poly(3,4-ethylenedioxythiophene):poly(4-styrene sulphonate) (PEDOT:PSS) [7]. As a result, a large energy barrier for hole injection exists, which is detrimental for the PLED performance. To enhance hole injection and transport, PFs are often copolymerized with hole-transport units (HTU) (called guests) like arylamines, and hole mobilities up to  $3 \times 10^{-7} \text{ m}^2/\text{Vs}$  have been reported in these copolymers [8]. An important issue is the alignment of the energy level of the host PF polymer and the arylamine based HTU. More specifically, the HOMO levels for PSF and  $N, N, N', N'$  tetraaryldiamino biphenyl (TAD) has been reported at  $-5.6 \text{ eV}$  and  $-5.4 \text{ eV}$ , respectively [9,10]. This energy offset between the PSF host copolymer and TAD guest HTU strongly affects the mobility of the holes since they tend to localize in the lower energy sites. At low concentrations the HTUs act as trapping sites for holes, thus limiting hole transport; on the other hand, when the number of guest units exceeds a critical value (typically 3–10%) [11–13], transport from guest to guest becomes possible, and the transport is further enhanced with increasing guest concentration.

In a recent paper, Nicolai *et al.* [14] have shown that the hole transport in the PSF polymer as well as in the host-guest PSF-TAD copolymers with guest concentrations ranging from 5–12.5 molar percent is trap-free space-charge-limited transport. For the PSF-TAD copolymer, the guest-guest hole transport could be described by the extended Gaussian disorder model (EGDM), with a density of hopping sites proportional to the TAD density and comparable to the molecular density. The electron transport was only studied in a PSF-10% TAD copolymer, and a free electron mobility in the  $\sim 10^{-9} \text{ m}^2/\text{Vs}$  regime was found. Since the lowest unoccupied molecular orbital (LUMO) of PSF is  $-2.6 \text{ eV}$  [15] and the LUMO of the

TAD HTU is  $-2.2$  to  $-2.4$  eV [16], the TAD unit cannot act as an electron trapping center. As a result, it is expected that the electron transport is not changed by the addition of TAD units. With the present level of understanding of PLEDs, and with the electron and hole transport of PSF-TAD copolymers known from single carrier devices, it should be possible to predict the effect of the addition of a HTU on the efficiency of the PSF-TAD PLED. This would be a case of truly predictive PLED device modeling. Here we study the charge transport properties of the blue-emitting PSF host as a reference as well as host-guest copolymers, where PSF is copolymerized with different percentages of the HTU (5-7.5-10-12.5% TAD). With the charge transport parameters known, we theoretically and experimentally study the operation of the respective PLEDs to find out which TAD concentration gives an optimal performance.

## II. CHARGE TRANSPORT IN HOST PSF POLYMER

Polymer light-emitting diodes and single carrier devices were fabricated on glass substrates with a patterned ITO layer. The substrates were cleaned, dried, and treated with ultraviolet (UV)-ozone. The polymer layers were spin-coated in a nitrogen atmosphere from a toluene solution. To measure the electron transport, the polymer layer was sandwiched between Al (30 nm) and Ba/Al (5/100 nm) contacts on a glass substrate deposited by thermal evaporation (chamber pressure  $\sim 10^{-6}$  mbar). The structure of the hole-only devices is glass/ITO/PEDOT:PSS/polymer/MoO<sub>3</sub>/Al. If the HOMO level of the polymer is around  $\sim -5.3$  eV, hole injection from PEDOT:PSS (Clevios P VP Al 4083 supplied by H. C. Starck) is still Ohmic, and the  $J$ - $V$  curves are symmetric, since MoO<sub>3</sub> is Ohmic even for polymers with a HOMO at  $\sim -6$  eV. If the HOMO level is deeper than  $-5.3$  eV, PEDOT:PSS cannot inject holes efficiently due to the injection barrier, whereas MoO<sub>3</sub> still provides an Ohmic contact, resulting in an asymmetric  $J$ - $V$ . In this way we can verify if PEDOT:PSS is still a good contact for the host-guest systems under study, which was the case. Because of this, in the ambipolar PLED we used the structure ITO/PEDOT:PSS/polymer/Ba/Al.

To investigate the PSF-TAD host-guest systems (shown in Fig. 1) in a systematic way, we start with the investigation of the host PSF polymer itself (0% TAD). Single carrier diodes, both electron-only and hole-only as well as double carrier PLEDs, were fabricated and characterized by steady-state

current-voltage measurements. Figure 2(a) shows the hole transport for a PSF hole-only device with 300 nm thickness at different temperatures. The hole transport was modeled using the EGDM as developed by Pasveer *et al.* [17]. In this model the effect of temperature, charge carrier density, and electric field on the charge transport are taken into account. The EGDM has three main parameters:  $\hat{\sigma} = \sigma/k_B T$  ( $k_B$ , Boltzmann constant), the normalized Gaussian disorder variance of energy of sites;  $a$ , the site spacing value (lattice constant or hopping parameter); and  $\mu_0$ , a mobility prefactor. The zero-field mobility is defined as  $\mu_0(T) = \mu_0 c_1 \exp(-c_2 \hat{\sigma}^2)$  with  $c_1 = 1.8 \times 10^{-9}$  and  $c_2$ , typically in the range 0.42–0.47 [14]. In our simulations we used for  $c_2$  the value 4/9 (0.444). Experimental data were simulated using a drift-diffusion model with the EGDM mobility embedded [18]. For the PSF host polymers, the parameters  $\mu_0 = 1800 \text{ m}^2/\text{Vs}$ ,  $a = 1.6 \text{ nm}$ , and  $\sigma = 0.14 \text{ eV}$  consistently describe the hole transport. At room temperature, the zero-field hole mobility then amounts to  $4 \times 10^{-12} \text{ m}^2/\text{Vs}$ . Opposite to the hole transport the electron transport is trap limited. When there are traps in the band gap that are distributed in energy, the slope of the  $\log J$ - $\log V$  will become steeper, and its magnitude will then depend on the shape of the energetic distribution ( $J \sim \frac{V^{m+1}}{L^{2m+1}}$ ). For the electron currents shown here, the slope is typically 5–6, indicative of severe trapping, as shown in Fig. 2(b). Next to the slope of  $\log J$ - $\log V$ , the dependence on sample thickness will also become stronger, and this enhancement is linked to the slope of the  $\log J$ - $\log V$ . In this way it can be verified that a current is trap-limited; it has been earlier reported that in PSF polymers the free electron mobility is at least an order of magnitude higher than the hole mobility [19]. Here the electron transport is modeled using a Gaussian trap distribution, with parameters  $E_t$  and  $\sigma_t$  the depth below the LUMO and width, respectively. The electron transport is well described using, for the free electron mobility, the EGDM parameters  $\mu_0 = 45\,000 \text{ m}^2/\text{Vs}$ ,  $a = 1.6 \text{ nm}$ , and  $\sigma = 0.14 \text{ eV}$  in combination with a trap density of  $3 \times 10^{23} \text{ m}^{-3}$ , a trap depth of 0.65 eV below the LUMO, and a width of the trap distribution of 0.10 eV.

As a next step the parameters derived from hole and electron transport were used to model the double carrier PSF PLED device. Figure 2(c) shows the temperature-dependent double carrier  $J$ - $V$  characteristic with a thickness of 300 nm. For the modeling, both radiative and nonradiative recombination mechanisms were taken into account. Radiative bimolecular recombination in organic semiconductors is of the Langevin

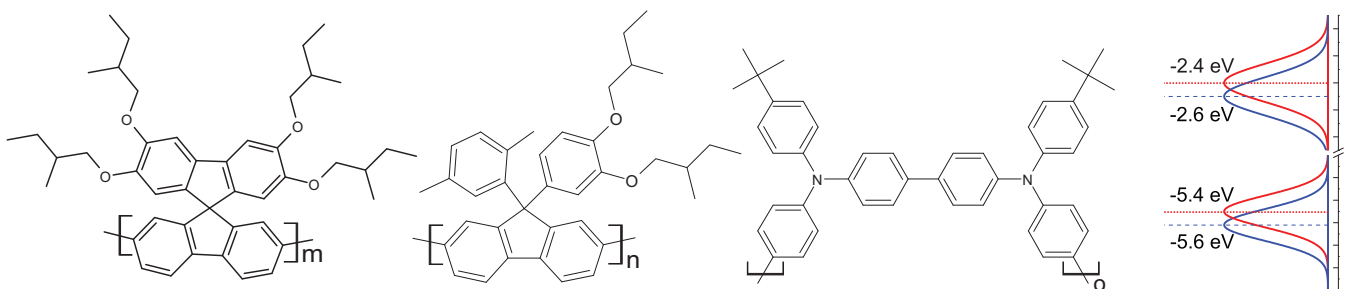


FIG. 1. (Color online) Chemical structure of PSF host copolymer and TAD HTU. The pristine copolymer PSF contains 50% of  $m$  and  $n$ , respectively. In the PSF-TAD copolymer with the TAD concentration ranging from 5–12.5%, the TAD unit is replacing the  $n$  part of the PSF host. In the energy diagram, the blue and red colors indicate the energy levels of PSF and TAD, respectively.

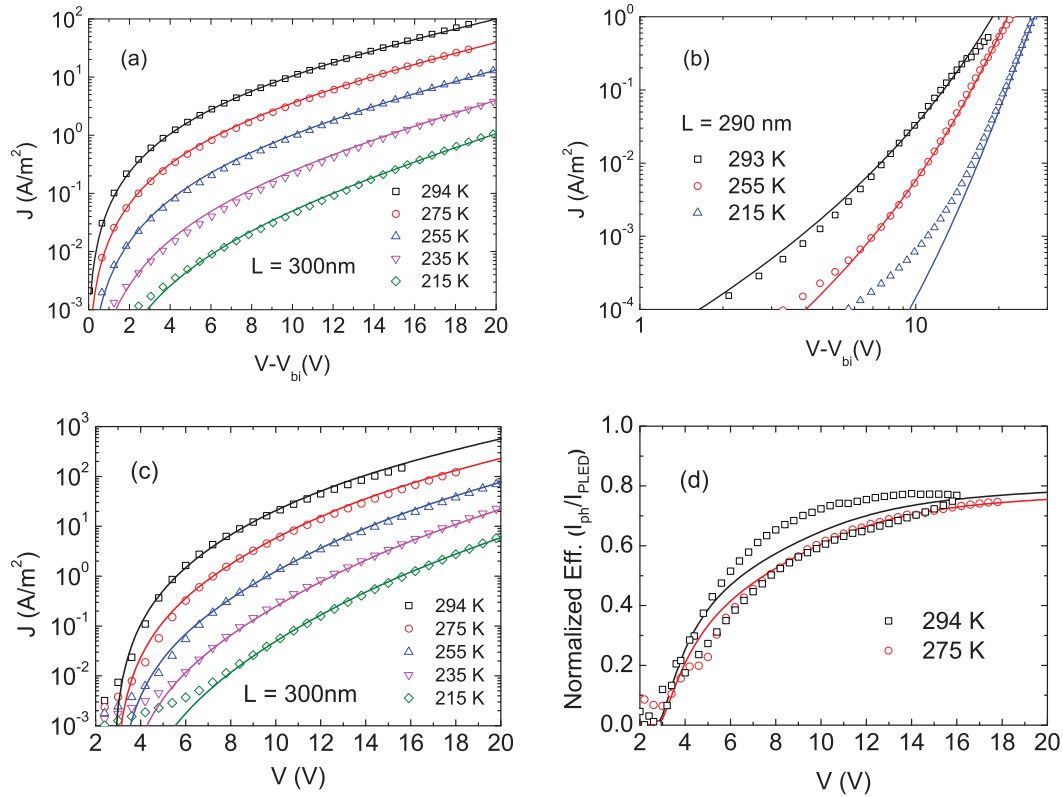


FIG. 2. (Color online) (a)  $J$ - $V$  characteristic of hole-only device of PSF,  $L = 300$  nm; (b)  $J$ - $V$  characteristic of electron-only device of PSF,  $L = 290$  nm; (c)  $J$ - $V$  characteristic of double carrier device,  $L = 300$  nm; (d) normalized current efficiency of device at two temperatures ( $I_{ph}/I_{PLED}$ ). Symbols are experimental data; lines are simulations.

type, i.e., the rate limiting step is the diffusion of free electrons and free holes toward each other in their mutual Coulomb field. The nonradiative recombination process is a trap-assisted recombination or Shockley-Read-Hall (SRH) recombination of free holes with trapped electrons. This is a two-step process where a trap state, originating from imperfections or impurities, with an energy level inside the forbidden energy band gap captures a charge carrier that subsequently recombines with a mobile carrier of the opposite sign because of their Coulombic interaction. Due to conservation of momentum, this process cannot occur without the release of a phonon slowing the recombination process down. Therefore, in most cases the trap sites act as recombination centers for nonradiative recombination. As a result the relative strengths of Langevin and SRH recombination determine the efficiency of an organic light-emitting diode (OLED). As recently reported by Kuik *et al.* [20], SRH recombination in organic semiconductors is given by

$$R_{SRH} = \frac{C_n C_p N_t (np - n_i^2)}{[C_n(n + n_1) + C_p(p + p_1)]}, \quad (1)$$

with the capture coefficients for electrons and holes  $C_n$  and  $C_p$ , respectively, given by

$$C_n = \frac{q}{\varepsilon} \mu_n, \quad C_p = \frac{q}{\varepsilon} \mu_p. \quad (2)$$

Langevin recombination is given by

$$R_L = \frac{q}{\varepsilon} (\mu_n + \mu_p) (np - n_i^2), \quad (3)$$

with  $q$  being the electron charge,  $\varepsilon$  the dielectric constant,  $\mu_n$  and  $\mu_p$  the electron and hole mobilities,  $n$  and  $p$  the free electron and hole densities, and  $n_i$  the intrinsic carrier concentration. Figure 2(c) shows that the double carrier current is very well reproduced from the transport data of the single carrier devices. Finally, we also look at the efficiency of the PSF PLED, here defined as light output divided by current and normalized to the maximum of the calculated current efficiency, as shown in Fig. 2(d). In order to describe the rise of efficiency with voltage, quenching of excitons at the cathode also has to be taken into account [21,22]. Using an exciton diffusion length of 6.3 nm, a value that is common

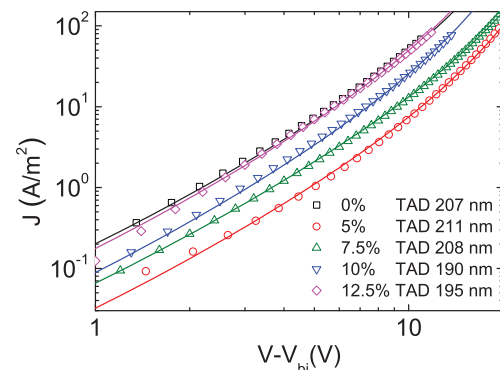


FIG. 3. (Color online)  $J$ - $V$  characteristics of hole-only devices of 0–12.5% TAD. Symbols are experimental data; lines are simulations.

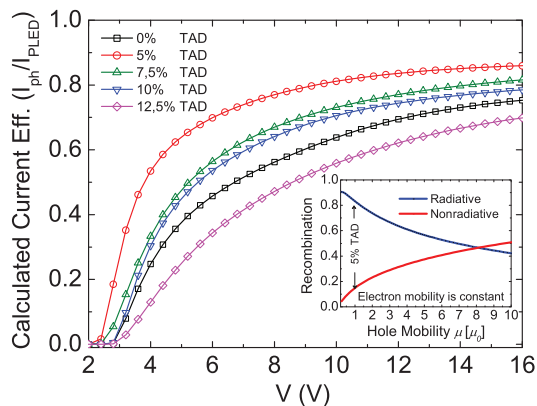


FIG. 4. (Color online) Calculated efficiency (light-output/current) for 300 nm PLEDs with varying concentration of TAD HTUs; The inset shows the relative contribution of radiative and nonradiative recombination vs hole mobility (normalized to 5% TAD), with the electron mobility assumed constant.

for conjugated polymers [23,24], the voltage dependence of the efficiency is well described. As a result, the reference PSF-based PLED is consistently described.

**A. Hole transport in host-guest copolymers**

As mentioned in the Introduction, Nicolai *et al.* [14] demonstrated that the hole transport in the PSF-TAD copolymers is in the guest-guest regime, and 5–12.5% TAD polymers are well-described using the EGDM. The site density  $N_t$  was found

to be proportional to the TAD concentration and reasonably close to the actual molecular site density. Furthermore, the disorder parameter  $\sigma$  (0.14 eV) was found to be essentially independent of the TAD concentration for all polymers, as expected for sufficiently dilute systems.

Figure 3 summarizes the  $J$ - $V$  characteristics of all hole-only devices for 0–12.5% TAD copolymers with thickness around 200 nm. As is clear from the figure for the 5% TAD copolymer, the mobility drops nearly an order of magnitude as compared to the reference (0% TAD). This is reflected in a change of the EGDM hole-transport parameter  $\mu_0$ , which ranges from 1800, 450, 950, 1100, and 2200  $\text{m}^2/\text{Vs}$  for 0%, 5%, 7.5%, 10%, and 12.5% TAD concentration, respectively. The disorder parameter  $\sigma$  was 0.14 eV for all copolymers, and the site spacing value was found to be in between 1.5–1.6 nm, similar to what was reported by Nicolai *et al.* [14].

Now with the hole transport known and the assumption that the electron transport will not change upon incorporation of TAD HTUs, we can predict the behavior of all PLEDs with varying TAD concentration. Figure 4 shows the predicted efficiencies as a function of voltage for various TAD concentrations. We observed that the best performance is expected for a TAD concentration of 5%. In the host PSF polymer, the transport of electrons and holes is strongly unbalanced due to trapping of electrons. As a result the recombination is strongly localized in the region close to the cathode, giving rise to enhanced quenching of excitons. The hole current can now be reduced by adding TAD units since at low concentrations (<3%) they act as hole traps. At 5% TAD, HTUs guest-guest transport, meaning transport between the

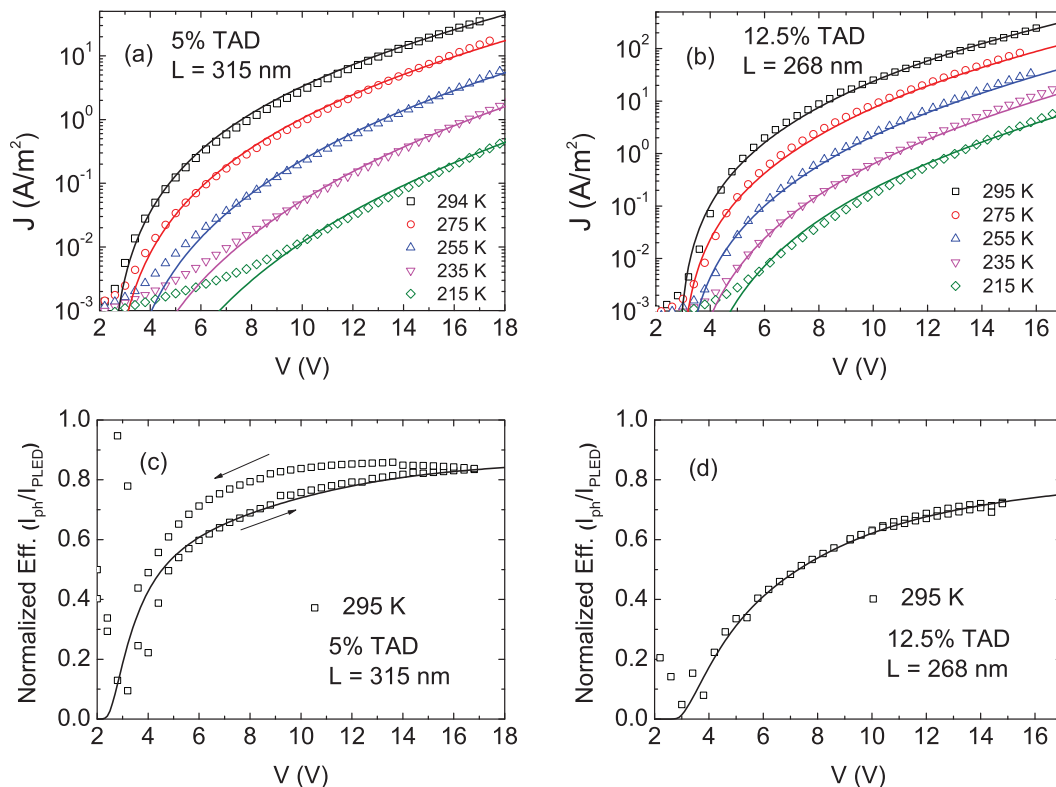


FIG. 5. (Color online) (a), (b)  $J$ - $V$  characteristics of 5 and 12.5% TAD polymers (polymers with lowest and highest amount of TAD). (c), (d) Normalized efficiency; symbols are experimental data and lines are calculations.



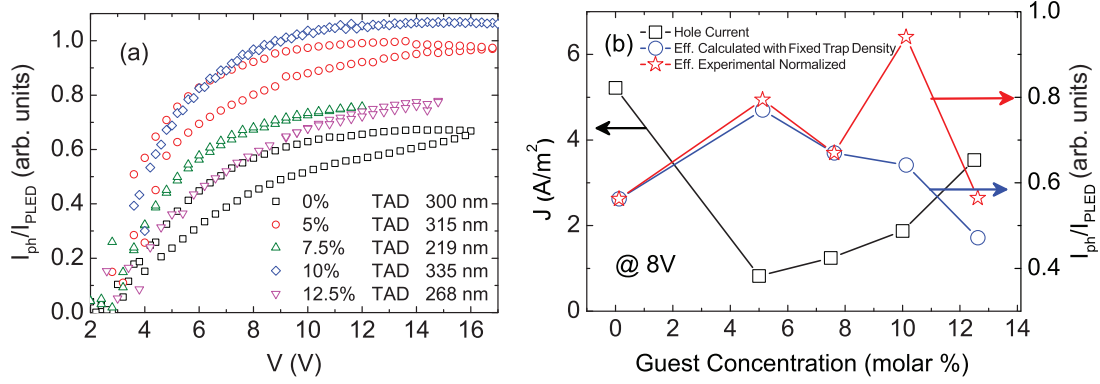


FIG. 6. (Color online) (a) Experimental (symbols) for  $\sim 300$  nm PLEDs with varying concentration of TAD HTUs. (b) Experimental efficiency at 8 V (stars) compared with predicted efficiency (circles) using a constant density of electron traps for the various polymers.

hole traps, becomes possible. However, due to the relatively low concentration of TAD units the guest-guest hole current is still significantly lower than the hole current in the host polymer. This reduction of the hole transport as compared to the host polymer then leads to a better balanced electron and hole transport and reduced exciton quenching at the cathode. Furthermore, as shown in the inset of Fig. 4, the ratio between nonradiative trap-assisted recombination and radiative bimolecular Langevin recombination is also strongly enhanced when the TAD concentration is increased from 5% to 12.5%. Since in the host PSF polymer the mobility of free electrons is already higher than the free hole mobility, a reduction of the hole mobility, as is the case for the polymer with 5% TAD, does not really influence the strength of the radiative Langevin recombination. This is, as can be seen from Eq. (3), because Langevin recombination is governed by the sum of the carrier mobilities, which is dominated by the electron mobility. On the other hand, the strength of the recombination of a free hole with a trapped electron, as can be estimated from Eq. (1) and Eq. (2) ( $R_{SRH} \sim q/\epsilon\mu_p N_t (np)$ ), is governed by the hole mobility only. Increasing the TAD concentration from 5% to 12.5% therefore leads to an enhancement of the trap-assisted recombination. For a TAD concentration around 11%, the efficiency is again equal to the one of the host polymer. Summarizing, our model calculations predict that a concentration of 5% TAD will lead to an optimum performance of the PLED. In the next section, this prediction will be experimentally validated.

### B. Performance validation of PSF-TAD PLEDs

As a first step we look at the charge transport properties of the double carrier PLEDs with the two extreme TAD concentrations of 5 and 12.5% TAD, respectively. As shown in Fig. 5, the predicted double carrier currents fit very well to the experimental data. This agreement also confirms that the electron mobility is indeed not changed by the incorporation of TAD units. Furthermore, as shown in Figs. 5(c) and 5(d), the efficiency is consistently described. It should be noted that the current efficiency of the host-guest polymer with 5% TAD [Fig. 5(c)] shows a counterclockwise hysteresis, and the calculations predict the forward up-scan behavior. This could point to the fact that at 5% concentration, some of the TAD units still act as an isolated hole trap. For

higher TAD concentrations, no hysteresis was observed. For completeness the data of the 7.5% and 10% TAD devices are given in the Supplemental Material [25]. As a next step we compare the (normalized) experimental efficiencies [Fig. 6(a)] as a function of TAD concentration. As shown in Fig. 6(b) for TAD concentrations of 5%, 7.5%, and 12.5%, the trend in the calculated efficiencies (stars) is exactly followed by the experiments (circles). Remarkably, the PSF LED with a 10% TAD concentration shows an almost twice as large efficiency as predicted. The major question now addresses why PLEDs of this 10% host-guest polymer are so much more efficient than the others. The only assumption made in the modeling was that the electron transport is not modified by the incorporation of the TAD HTUs. This assumption needs to be experimentally verified first.

### C. Electron transport in PSF-TAD polymers

As stated above, in all PSF-TAD copolymers the electron transport is trap-limited. In Fig. 7, the electron currents for the various PSF-TAD copolymers are shown. It should be noted that all devices have a thickness of around 200 nm, except the device with 5% TAD, which therefore exhibits a relatively low electron current. From the graph, it is observed that the polymer with 10% TAD exhibits a higher electron current than the other polymers, whereas the device with 7.5% TAD has the

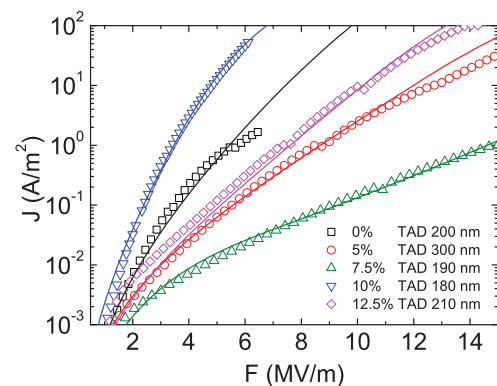


FIG. 7. (Color online)  $J$ - $F$  characteristic of electron-only devices of 0–12.5% TAD ( $F$  is applied field, voltage/(device thickness)). Symbols are experimental data; lines are simulations.

TABLE I. Electron transport parameters for 0–12.5% TAD host-guest polymer.

| Parameters                            | 0% TAD               | 5% TAD               | 7.5% TAD             | 10% TAD              | 12.5% TAD            |
|---------------------------------------|----------------------|----------------------|----------------------|----------------------|----------------------|
| $\mu_{p0}(\text{m}^2/\text{Vs})$      | 45000                | 45000                | 45000                | 45000                | 45000                |
| $a_n$ (nm)                            | 1.62                 | 1.65                 | 1.67                 | 1.68                 | 1.7                  |
| $\sigma_n$ (eV)                       | 0.14                 | 0.14                 | 0.14                 | 0.14                 | 0.14                 |
| $N_{t\text{gauss}} (\text{m}^{-3})$   | $3.0 \times 10^{23}$ | $4.0 \times 10^{23}$ | $4.7 \times 10^{23}$ | $1.3 \times 10^{23}$ | $3.0 \times 10^{23}$ |
| $E_{nt\text{gauss}} (\text{eV})$      | 0.65                 | 0.65                 | 0.65                 | 0.65                 | 0.65                 |
| $\sigma_{nt\text{gauss}} (\text{eV})$ | 0.1                  | 0.1                  | 0.1                  | 0.1                  | 0.1                  |

lowest electron current. As for the host polymer (0% TAD), the electron currents are modeled using a Gaussian distribution of trap states at 0.65 eV below the LUMO. We assume that the free electron mobility is not affected by the incorporation of TAD. The electron transport parameters then obtained are summarized in Table I.

Regarding the parameters for the free electron transport, we only have to slightly increase the hopping distance a bit, which is natural since the addition of HTU slightly dilutes the concentration of electron transport sites. The major change, however, is in the number of electron traps. The polymers with 0%, 5%, 7.5%, and 12.5% have an electron trap concentration in the range  $3\text{--}5 \times 10^{23} \text{ m}^{-3}$ , which is typical for conjugated polymers. The only exception is the 10% TAD material that has a trap concentration of a factor of three less.

A major question in the field of conjugated polymers is the microscopic origin of the electron traps. The fact that their concentration is similar, typically  $3\text{--}5 \times 10^{23} \text{ m}^{-3}$ , in a large range of conjugated polymers [1] indicates that the electron trapping in conjugated polymers has a common origin. The electron traps cannot result from structural defects like kinks, since different polymers have different stiffness, and some are crystalline or amorphous. A more likely origin is a chemical defect related to water or oxygen. Quantum-chemical calculations [1] showed that hydrated-oxygen complexes can provide electron trap sites with an energy corresponding to those measured, with the  $(\text{H}_2\text{O})_2\text{--O}_2$  complex as a likely candidate. Such a defect can already be incorporated during the synthesis of the polymers. Also, the PSF-TAD polymers investigated here have an electron trap density in the range  $3\text{--}5 \times 10^{23} \text{ m}^{-3}$ , except the one with 10% TAD. This polymer

has a reduced trap concentration of  $1.3 \times 10^{23} \text{ m}^{-3}$  that, although in the same order of magnitude, has a large influence on the PLED performance. This reduced electron trap concentration is taken into account in the calculated efficiency for the 10% TAD PLED, as shown in the Supplemental Material [Fig. S1(d) [25]]. As a next step we model the effect of a variation in trap concentration between 1 and  $5 \times 10^{23} \text{ m}^{-3}$  on the performance of the PSF-TAD PLEDs. The origin of the increased efficiency can already be seen in Fig. 8, where the emission profile is shown for the various polymers at a current density of  $50 \text{ A/m}^2$ .

At sufficiently high bias the recombination in the 10% TAD device shifts from cathode to anode due to filling of the reduced number of electron traps, leading to a reduction of exciton quenching at the cathode and enhanced efficiency. To address the effects of electron traps on the efficiency more quantitatively, we compare in Fig. 9 the loss processes in the 10% TAD polymer assuming an electron trap density of  $1.3 \times 10^{23} \text{ m}^{-3}$  and  $5 \times 10^{23} \text{ m}^{-3}$ , respectively. We observe that both the quenching at the cathode (as shown in Fig. 8) as well as the nonradiative SRH recombination via the electron traps are strongly reduced. The latter is a direct consequence of the reduced number of traps.

A major conclusion that can be drawn from this study is that predictive modeling of PLEDs is only possible when the quality of the materials is constant. Intrinsic effects as charge balance are easily overruled by variations in extrinsic defects. To exploit the benefits of predictive device modeling control of these impurities is therefore an absolute must.

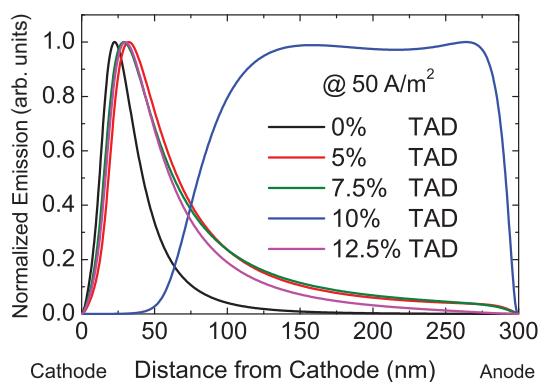


FIG. 8. (Color online) Calculated exciton density at a current density of  $50 \text{ A/m}^2$  as a function of position for PSF-TAD PLEDs with a thickness of 300 nm.

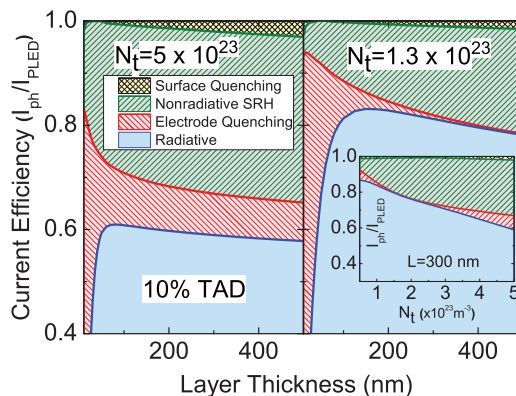


FIG. 9. (Color online) Calculated current efficiency for 10% TAD PLEDs at  $10 \text{ A/m}^2$  vs device thickness at high ( $5 \times 10^{23} \text{ m}^{-3}$ ) and low ( $1.3 \times 10^{23} \text{ m}^{-3}$ ) trap densities right and left, respectively. Inset shows the current efficiency evolution vs trap density.

### III. CONCLUSION

In conclusion, the hole and electron transport in a series of host-guest PSF-TAD (0%, 5%, 7.5%, 10%, and 12.5%) polymers were studied. From model calculations it was expected that a 5% TAD concentration would lead to an optimal performance of the PLED due to better balanced charge transport and reduction of nonradiative SRH recombination. Experimentally, it was observed that the PLED with 10% TAD units gave the best performance. Analysis of the charge transport showed that in the 10% TAD copolymer, the number of (extrinsic) electron traps was reduced by a factor of three to five compared to the other four copolymers, and that all exhibited the universal trap concentration in the  $3\text{--}5 \times 10^{23} \text{ m}^{-3}$  range. This reduced trap concentration leads to an enhanced electron transport such that at sufficient bias the

recombination for the 10% TAD device shifts from the cathode to the anode. For the other copolymers, the recombination stays pinned at the cathode. Furthermore, the reduced number of electron traps also leads to a decrease of nonradiative trap-assisted recombination. Combination of these two effects almost doubles the efficiency of the 10% TAD PLED as compared to the expected value.

### ACKNOWLEDGMENTS

Authors acknowledge Gert-Jan Wetzelaer for fruitful discussions and Jan Harkema for technical support. D.A. is supported by the Dutch Polymer Institute (DPI), Project No. 733. The PSF-TAD copolymers were supplied by Merck KGaA.

- 
- [1] H. T. Nicolai, M. Kuik, G. A. H. Wetzelaer, B. de Boer, C. Campbell, C. Risko, J. L. Brédas, and P. W. M. Blom, *Nat. Mater.* **11**, 882 (2012).
- [2] M. Kuik, G.-J. A. H. Wetzelaer, H. T. Nicolai, N. I. Craciun, D. M. De Leeuw, and P. W. M. Blom, *Adv. Mater.* **26**, 512 (2014).
- [3] M. Kuik, H. T. Nicolai, M. Lenés, G.-J. A. H. Wetzelaer, M. Lu, and P. W. M. Blom, *Appl. Phys. Lett.* **98**, 093301 (2011).
- [4] Q. Pei and Y. Yang, *J. Am. Chem. Soc.* **118**, 7416 (1996).
- [5] W. Grice, D. D. C. Bradley, M. T. Bernius, M. Inbasekaran, W. W. Wu, and E. P. Woo, *Appl. Phys. Lett.* **73**, 629 (1998).
- [6] W.-L. Yu, J. Pei, W. Huang, and A. J. Heeger, *Adv. Mater.* **12**, 828 (2000).
- [7] A. J. Campbell, D. D. C. Bradley, and H. Antoniadis, *J. Appl. Phys.* **89**, 3343 (2001).
- [8] M. Redecker, D. D. C. Bradley, M. Inbasekaran, W. W. Wu, and E. P. Woo, *Adv. Mater.* **11**, 241 (1999).
- [9] L.-B. Lin, R. H. Young, M. G. Mason, S. A. Jenekhe, and P. M. Borsenberger, *Appl. Phys. Lett.* **72**, 864 (1998).
- [10] F. Laquai and D. Hertel, *Appl. Phys. Lett.* **90**, 142109 (2007).
- [11] D. M. Pai, J. F. Yanus, and M. Stolka, *J. Phys. Chem.* **88**, 4714 (1984).
- [12] R. J. de Vries, S. L. M. van Mensfoort, V. Shabro, S. I. E. Vulto, R. A. J. Janssen, and R. Coehoorn, *Appl. Phys. Lett.* **94**, 163307 (2009).
- [13] I. Fishchuk, A. Kadashchuk, A. Vakhnin, Y. Korosko, H. Bäessler, B. Souharce, and U. Scherf, *Phys. Rev. B* **73**, 115210 (2006).
- [14] H. T. Nicolai, A. J. Hof, M. Lu, P. W. M. Blom, R. J. de Vries, and R. Coehoorn, *Appl. Phys. Lett.* **99**, 203303 (2011).
- [15] M. C. Gather, F. Ventsch, and K. Meerholz, *Adv. Mater.* **20**, 1966 (2008).
- [16] <http://www.sigmaaldrich.com/catalog/product/aldrich/443263?lang=en&region=NL> (27 October 2014).
- [17] W. F. Pasveer, J. Cottaar, C. Tanase, R. Coehoorn, P. A. Bobbert, P. W. M. Blom, D. M. de Leeuw, and M. A. J. Michels, *Phys. Rev. Lett.* **94**, 206601 (2005).
- [18] L. J. A. Koster, E. C. P. Smits, V. D. Mihailetschi, and P. W. M. Blom, *Phys. Rev. B* **72**, 085205 (2005).
- [19] H. T. Nicolai, A. Hof, J. L. M. Oosthoek, and P. W. M. Blom, *Adv. Funct. Mater.* **21**, 1505 (2011).
- [20] M. Kuik, L. J. A. Koster, G. A. H. Wetzelaer, and P. W. M. Blom, *Phys. Rev. Lett.* **107**, 256805 (2011).
- [21] M. Kuik, L. J. A. Koster, A. G. Dijkstra, G. A. H. Wetzelaer, and P. W. M. Blom, *Organic Electronics* **13**, 969 (2012).
- [22] O. V. Mikhnenko, M. Kuik, J. Lin, N. van der Kaap, T.-Q. Nguyen, and P. W. M. Blom, *Adv. Mater.* **26**, 1912 (2014).
- [23] D. E. Markov, J. C. Hummelen, P. W. M. Blom, and A. B. Sieval, *Phys. Rev. B* **72**, 045216 (2005).
- [24] D. E. Markov, C. Tanase, P. W. M. Blom, and J. Wildeman, *Phys. Rev. B* **72**, 045217 (2005).
- [25] See Supplemental Material at <http://link.aps.org/supplemental/10.1103/PhysRevB.90.205204> for the  $J$ - $V$  characteristic of a double carrier device with 7.5% and 10% TAD guest units.